Development 139, 2966-2977 (2012) doi:10.1242/dev.079632

BCDO2 acts as a carotenoid scavenger and gatekeeper for the mitochondrial apoptotic pathway

Glenn P. Lobo[1], Andrea Isken[2,*], Sylvia Hoff[1,2,‡], Darwin Babino[1] and Johannes von Lintig[1,§]

SUMMARY

Carotenoids and their metabolites are widespread and exert key biological functions in living organisms. In vertebrates, the carotenoid oxygenase BCMO1 converts carotenoids such as β,β-carotene to retinoids, which are required for embryonic pattern formation and cell differentiation. Vertebrate genomes encode a structurally related protein named BCDO2 but its physiological function remains undefined. Here, we show that BCDO2 is expressed as an oxidative stress-regulated protein during zebrafish development. Targeted knockdown of this mitochondrial enzyme resulted in anemia at larval stages. Marker gene analysis and staining for hemoglobin revealed that erythropoiesis was not impaired but that erythrocytes underwent apoptosis in BCDO2-deficient larvae. To define the mechanism of this defect, we have analyzed the role of BCDO2 in human cell lines. We found that carotenoids caused oxidative stress in mitochondria that eventually led to cytochrome c release, proteolytic activation of caspase 3 and PARP1, and execution of the apoptotic pathway. Moreover, BCDO2 prevented this induction of the apoptotic pathway by carotenoids. Thus, our study identifying BCDO2 as a crucial protective component against oxidative stress establishes this enzyme as mitochondrial carotenoid scavenger and a gatekeeper of the intrinsic apoptotic pathway.

KEY WORDS: Carotenoids, Zebrafish, Mitochondria, BCDO2 (BCO2), Reactive oxygen species, Apoptosis

INTRODUCTION

Animals, including humans, metabolize carotenoids to apocarotenoids (such as retinaldehyde, the chromophore of G-protein-coupled receptors that mediate phototransduction) (Palczewski, 2006) and to all-trans-retinoic acid, a hormone-like compound that is crucial for processes as diverse as embryonic development, tissue homeostasis and immunity (Chambon, 1996; Agace, 2008). For carotenoid metabolism, vertebrate genomes encode two types of carotenoid-cleaving enzymes annotated as β-carotene-15,15′-monooxygenase (BCMO1) and β-carotene-9′,10′-dioxygenase (BCDO2, also named BCO2 and CMO2) (von Lintig, 2010). BCMO1 is the key enzyme for vitamin A production (Hessel et al., 2007) and converts a limited number of proretinoid carotenoids, such as β,β-carotene (BC), to retinaldehyde by symmetric cleavage at position C15,C15′ (Paik et al., 2001; Redmond et al., 2001; Lindqvist and Andersson, 2002). The second carotenoid-cleavage enzyme, BCDO2, displays broad substrate specificity towards various dietary carotenoids and catalyzes an eccentric oxidative cleavage at position C9′,C10′, resulting in the production of apocarotenoids different from retinoids (Hu et al., 2006; Mein et al., 2010; Amengual et al., 2011). There is also a marked difference in the subcellular localization of these two vertebrate carotenoid-oxygenases. BCMO1 is a cytoplasmic protein (Lindqvist and Andersson, 2002), whereas BCDO2 localizes to mitochondria (Amengual et al., 2011).

[1]Case Western Reserve University, School of Medicine, Department of Pharmacology, 10900 Euclid Avenue, Cleveland, OH 44106, USA. [2]Albert-Ludwigs Universitaet Freiburg, Institut fuer Biologie 1, Hauptstrasse 1, 79104 Freiburg, Germany.

*Present address: Novartis Pharma AG, Basel, Switzerland
‡Present address: Molecular Biology Department of Nephrology, University Medical Center, Freiburg, Germany
§Author for correspondence (johannes.vonlintig@case.edu)

Accepted 22 May 2012

Though the biochemical function of BCDO2 as carotenoid cleavage enzyme is now well established, its physiological role is controversial. On the one hand, several studies propose that BCDO2 catalyzes the first step in pathways for the production of biologically active apocarotenoid signaling molecules (Lian et al., 2007; Ford et al., 2011). Such compounds are widespread in living organisms, e.g. in plants, and regulate important physiological responses (Moise et al., 2005). On the other hand, studies in *Bcdo2* knockout mice implicate BCDO2 in carotenoid catabolism and homeostasis. When challenged with artificial diets, carotenoids accumulated in mutant animals and induced oxidative stress (Amengual et al., 2011). Vertebrates show significant differences in carotenoid metabolism and functions. Rodents such as mice display low to undetectable levels of these compounds in blood and tissues (Hessel et al., 2007; Amengual et al., 2011), indicating that they have developed mechanisms to prevent carotenoid accumulation. Indeed, recent research revealed that intestinal carotenoid absorption is under negative-feedback regulation by vitamin A (Lobo et al., 2010b) and that non-proretinoid carotenoids are rapidly metabolized by BCDO2 (Ford et al., 2010; Amengual et al., 2011). By contrast, many mammals, including humans, and oviparous vertebrates, such as birds and fish, have significant levels of carotenoids in blood and tissues. These carotenoids exert important physiological functions as colorants, antioxidants and filters of phototoxic blue light in the eyes, and are involved in the immune response (Bone et al., 2000; Blount et al., 2003; Krinsky et al., 2003). Thus, the issue arises as to whether BCDO2 functions are conserved between rodents and other members of the vertebrate kingdom.

To study carotenoid metabolism in such vertebrates, lower primates, gerbils and ferrets were used as models in several studies (Lee et al., 1999). But a major flaw in the use of these animals for research is the lack of manageable and cost-efficient protocols for their genetic manipulation. To overcome this problem and to further elucidate the role of BCDO2 in carotenoid metabolism, we took advantage of the zebrafish model (*Danio rerio*) and human

cell lines, both systems being highly suited for genetic and pharmacological manipulation (Lieschke and Currie, 2007). More importantly for this study, carotenoids are crucial for zebrafish development and the egg yolk contains significant amounts of these compounds that must be mobilized and distributed during embryogenesis (Lampert et al., 2003).

MATERIALS AND METHODS

Materials

All chemicals, unless stated otherwise, were purchased from Sigma-Aldrich (St Louis, MO). Canthaxanthin and β,β-carotene (BC) were purchased from Wild (Germany).

Test for enzymatic activity

Full-length zebrafish *bcdo2* cDNA (GenBank Accession Number AJ290391.1) was cloned into the expression vector pTRChis (Invitrogen, Carlsbad, CA). The plasmid was transfected into an *E. coli* strain capable of synthesizing BC and assays were performed as described previously (von Lintig and Vogt, 2000). For tests of enzymatic activity, murine BCDO2 was expressed as a recombinant protein in *E. coli* analyzed with canthaxanthin (Wild, Germany) and 4-oxo-N-(4-hydroxyphenyl)-all-trans-retinamide (4-oxo-4HPR) (Research Chemicals, Toronto, Canada) as previously described (Amengual et al., 2011).

Zebrafish strains and maintenance

Zebrafish (strain AB/TL) were bred and maintained under standard conditions at 28.5°C. Morphological features were used to determine the stage of the embryos in hours (hpf) or days (dpf) post fertilization. Embryos used for in situ hybridization were raised in the presence of 200 μM 1-phenyl-2-thiourea (PTU).

Whole-mount in situ hybridization

Whole-mount in situ hybridization was performed according to published protocols (Isken et al., 2008). *Bcdo2* was cloned into the vector pCRII-TOPO (Invitrogen, Grand Island, NY), and antisense RNA probes were synthesized as outlined by the manufacturer (Roche Applied Sciences, Indianapolis, IN). Additional RNA probes used for in situ hybridization experiments were for *gata1*, *gata2*, and *hbae3*.

Injections of morpholino oligonucleotides

For targeted knockdown of the BCDO2 protein, antisense morpholino oligonucleotides (MO) (GeneTools) were designed that targeted bases –9 to +16 of *bcdo2* (*bcdo2*-MO1, 5′-TGTAGACATGACTTTAGG-TGTTATG-3′) and the splice acceptor site of exon 2/intron 3 (E2I3-MO2, 5′-TAGGTGTGACTTCTTACTTGCTTTC-3) of *bcdo2* mRNA. For controls, the standard morpholino oligonucleotides (GeneTools) were used (control-MO: 5′-GTATTGTGGATTTCAGTACAGATGT-3′). The injected volume was ~3 nl, corresponding to 5.1 ng of MO per embryo.

Treatments and staining of embryos

4-oxo-4HPR was prepared from stocks in dimethyl sulfoxide and applied to achieve a 1 μM concentration in egg water. The terminal deoxynucleotidyl transferase dUTP nick end labeling (TUNEL) assay was performed with the In Situ Cell Death Detection Kit, TMR Red (Roche Applied Sciences, Indianapolis, IN). o-Dianisidine staining of zebrafish embryos was performed according to published protocols (Isken et al., 2008).

Cell lines and culture

COS7 monkey kidney cells, HepG2 human liver carcinoma cells, Hek293 human embryonic kidney cells and NIH-3T3 mouse embryo fibroblasts cells were maintained in high-glucose DMEM, whereas human breast carcinoma MDA231, T47D and BT549 cells were maintained in RPMI media, supplemented with 10% fetal bovine serum (FBS). Cells were cultured in a 37°C humidified CO_2 incubator. Cytochrome c and COX IV endogenous protein co-localization studies and treatment with carotenoids were performed as previously described (Amengual et al., 2011).

RNA isolation and quantitative real-time PCR (qRTPCR) analysis

RNA was isolated from zebrafish embryos (± indicated treatments) and cultured cells with the Trizol reagent (Invitrogen, Grand Island, NY), and purified with the RNeasy system (Qiagen, Valencia, CA). Quantitative real time PCR (Q-RTPCR) was carried out with TaqMan chemistry, namely TaqMan Gene Expression Master Mix and Assays on Demand probes (ABI) for zebrafish *bcdo2* (Dr03144457_m1), *gpx1* (Dr03071768_m1), *catalase* (Dr03099094_m1) and *hbbe3* (Dr03090427_m1).

Histological methods

Measurement of mitochondrial membrane potential (ΔΨm) in HepG2 and T47D cells after carotenoid treatment was carried out as outlined by the manufacturer (ImmunoChemistry Technologies, Bloomington, MN). Staining for reactive oxygen species (ROS) was carried out with the Image-iT LIVE ROS kit (Molecular Probes, Invitrogen). Chromatin condensation in cell lines was evaluated by using the DNA vital dye, Hoechst 33342. All experiments were carried out in duplicate and repeated three times. About 50-60 cells from 10-12 fields were analyzed per experiment.

Small-interfering RNA preparation and transfection

bcdo2 small-interfering RNA [FlexiTube siRNA Premix: Qiagen (Valencia, CA)], a target-specific 19 nucleotide siRNA set (pre-validated pool of four individual siRNAs) designed to knock down *bcdo2* expression, was used to silence Bcdo2 expression. Cells in the exponential phase of growth were seeded in six-well plates at a concentration of 5×10^5 cells/well. Twenty-four hours later they were transfected with siRNA specific for *bcdo2* and non-targeting siRNA at a final concentration of 100 nM according to the manufacturer's protocol. Silencing of *bcdo2* was examined 72 hours after transfection.

Microscopy

Fluorescent images were obtained by using a Zeiss LSM 510 UV Meta confocal microscope with an HCX Plan 63× numerical aperture 1.4 oil-immersion objective lens. Images were acquired with Zeiss confocal software, version 2.0, or with an Axioplan 2 fluorescence microscope (GFP filter set: excitation 473, emission 520; Samrock, Rochester, NY) with a Zeiss AxioCam MR camera at 10× magnification.

Statistical analyses

Results are presented as mean±s.d. and the number of experiments is indicated in the figure legends. All determinations for each experiment were performed at least in triplicate. Statistical significance was assessed by using the two-tailed Student's *t*-test.

RESULTS

Zebrafish BCDO2 biochemistry and cellular localization

We previously cloned a *bcdo2* cDNA (annotated as β-carotene-15,15′-dioxygenase 2, like *bcdo2l*) from this fish and showed that zebrafish egg yolk contains carotenoids (Kiefer et al., 2001; Lampert et al., 2003). To determine the subcellular localization of the enzyme, we expressed zebrafish BCDO2 as V5-tagged protein in COS7 cells. Immunostaining and confocal imaging revealed that BCDO2 was distributed in cells in a pattern resembling that expected for mitochondria (Fig. 1A). Therefore, we performed co-immunostaining for cytochrome c oxidase IV (COXIV), a mitochondrial marker protein. Merged images showed that BCDO2 colocalized with COXIV, suggesting a mitochondrial localization for this enzyme (Fig. 1A). We next expressed zebrafish BCDO2 in an *E. coli* strain capable of synthesizing BC. We have previously established this system to assess the activity of carotenoid oxygenases from various organisms (von Lintig and Vogt, 2000) and BC is the major carotenoid in the zebrafish egg yolk (Lampert et al., 2003). HPLC analyses of lipid extracts from this *E. coli* strain showed that an apocarotenoid product was formed upon expression of zebrafish BCDO2 that evidenced a similar retention

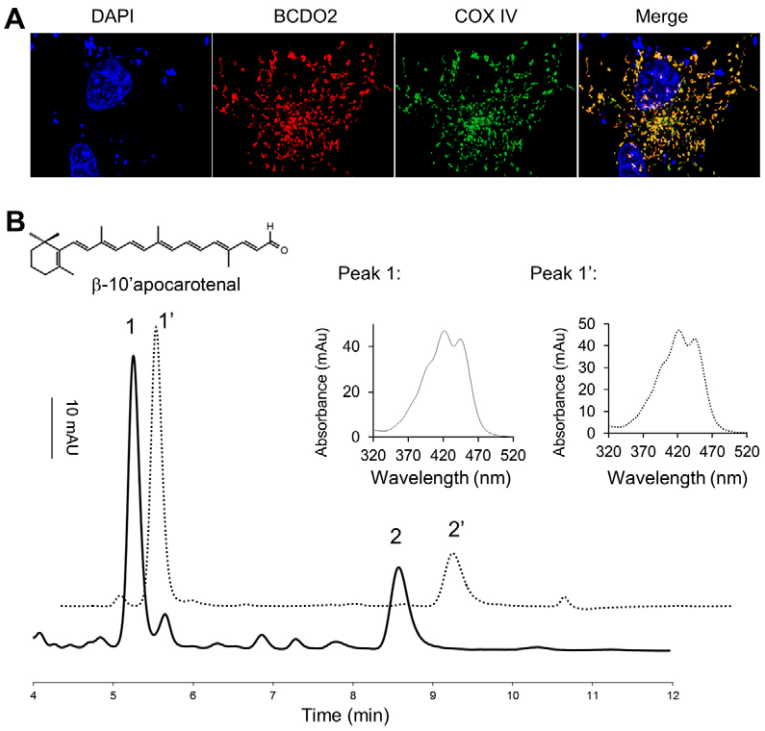

Fig. 1. Subcellular localization and biochemical properties of zebrafish BCDO2. (**A**) COS7 cells expressing recombinant zebrafish BCDO2 with a V5 tag. Immunostaining was performed using anti-V5 antibody for BCDO2 (red) and mitochondria-specific anti-COXIV antibody (green). Merged image (right-most panel) shows mitochondrial colocalization of BCDO2 with COXIV. Images are taken at 63× magnification. (**B**) Recombinant zebrafish BCDO2 was expressed in an *E. coli* strain capable of synthesizing BC. Carotenoids and putative carotenoid-cleavage products were extracted and subjected to HPLC analysis. The solid line shows a HPLC profile at 420 nm of the *E. coli* lipid extract. Two major peaks (1 and 2) became detectable. These peaks showed similar retention times and spectral characteristics (insets) as the β-10′-apocarotenal oxime (*syn* and *anti*) standards (peaks 1′ and 2′) (dotted line). The insets give spectral characteristics of peak 1 and peak 1′.

time and spectral characteristics to the β-10′-apocarotenal standard (Fig. 1B). Thus, we demonstrated that the zebrafish *bcdo2* gene encoded a mitochondrial carotenoid-9′,10′-oxygenase.

bcdo2 is expressed in the developing zebrafish

Using whole-mount in situ hybridization, we next analyzed the expression pattern of *bcdo2* during development (Fig. 2). *bcdo2* mRNA expression became detectable during segmentation in ventral cell layers of the head and trunk (Fig. 2A). At 24 hours post fertilization (hpf), *bcdo2* mRNA expression in ventral cell layers became more restricted to anterior regions of the embryo (Fig. 2B,C). Beginning at 32 hpf, *bcdo2* mRNA became detectable in the pericardial region (Fig. 2D,E). At 48 hpf, cells of the atrium and the ventricle also expressed *bcdo2* as confirmed in cross-sections (Fig. 2F-I). At 3 and 4 days post fertilization (dpf), liver and gut cells also expressed *bcdo2* (Fig. 2J-L).

Knock down of *bcdo2* causes anemia

To address the requirement of *bcdo2* for development, we disrupted its function by targeted gene knock down with antisense morpholino oligonucleotides (MO) (Nasevicius and Ekker, 2000). MO1 was directed against the 5′-region of *bcdo2* mRNA and MO2 was directed against the splice acceptor site of exon 2 (supplementary material Fig. S1A). After injection of the MO1 into eggs at the one-cell stage, we confirmed efficient targeted knockdown of BCDO2 by immunoblot analysis with a polyclonal antiserum raised against murine BCDO2 (Fig. 3G) (Amengual et al., 2011). By RT-PCR analysis, we also demonstrated that MO2 interfered with *bcdo2* mRNA splicing (supplementary material Fig. S1B,C). Morphants showed no gross patterning defects or obvious malformations of organ systems such as the eyes and brain. On closer microscopic inspection, we noted that the blood in *Bcdo2* morphants was no longer red-colored as in control embryos (Fig. 3A-D; supplementary material Fig. S1D). In 3 dpf MO1-treated morphants, the filling of the heart with blood cells was reduced (Fig. 3E,F).

BCDO2 deficiency induces blood cell apoptosis at larval stages

To investigate whether BCDO2 is required for erythropoiesis, we analyzed the expression pattern of the hematopoietic transcription factors *gata1* and *gata2*. Genetic disruption of *gata1* results in a reduction of mature erythrocytes as demonstrated in mouse and zebrafish mutants (Pevny et al., 1991). However, the expression of both these marker genes was unaltered in zebrafish morphants when compared with controls (Fig. 4A-F), indicating that primitive erythropoiesis and the proliferation erythroid progenitor cells was not affected. Furthermore, embryonic α-globin (*hbae3*), a late marker of erythrocyte differentiation, appeared to be expressed in morphants at 2 dpf (Fig. 4M,N). We next performed staining for hemoglobin by using o-Dianisidine with staged embryos. This analysis revealed that erythrocytes were present in morphants and controls at 2 dpf (Fig. 4G,H). But at 3 and 4 dpf, this picture changed such that a strong reduction of o-Dianisidine stainable cells was noted in morphants (Fig. 4I-L). Blood smears of 3 dpf larvae showed that erythrocytes of morphants exhibited fragmented nuclei, indicating that these cells had undergone apoptosis (Fig. 4O,P). To verify this assumption, we then performed TUNEL staining with 2 dpf *bcdo2* morphants and wild-type siblings. Importantly, this staining indicated a large number of TUNEL-positive blood cells in morphants that accumulated in the region where the caudal hematopoietic tissue develops (Murayama et al., 2006; Jin et al., 2007) (Fig. 4Q,R). This region is colonized by hematopoietic stem cells at this developmental time point and provides a niche for blood cell differentiation (Ellett and Lieschke, 2010; Stachura and Traver, 2011). The large amount of TUNEL-positive cells in this region indicated that these differentiating blood cells were most sensitive to apoptosis in BCDO2 deficiency.

Previously, it has been shown that PTU can exacerbate anemia in fish larvae (Yu et al., 2010). Hence, we also raised *bcdo2* morphants in the absence of this compound. At 3 dpf, *bcdo2* morphants showed reduced staining for hemoglobin and

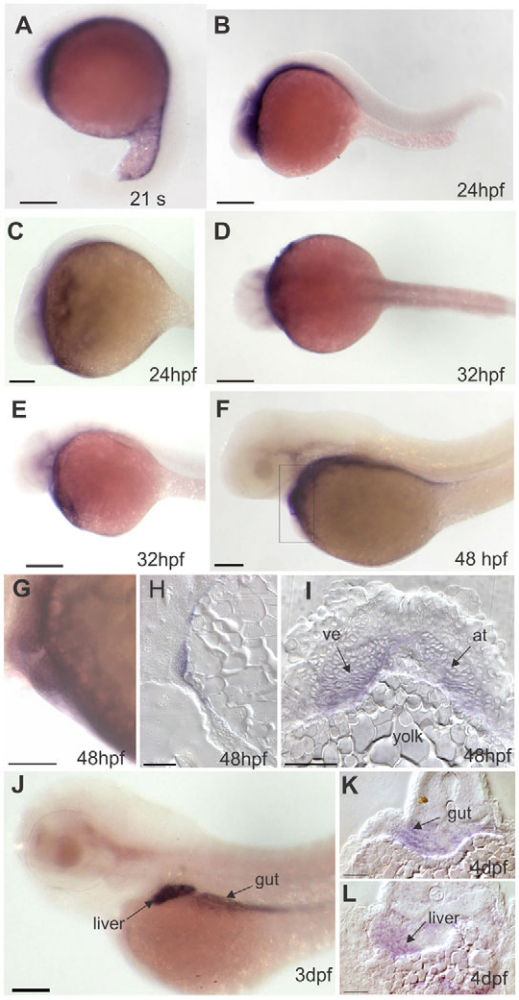

Fig. 2. Expression patterns of *bcdo2* during zebrafish development. (A-C,E-G,K) Lateral views, anterior is leftwards. (D) Dorsal view (anterior is leftwards; (H) sagittal section; (I,K,L) transverse cross-sections. (**A**) During late segmentation stages, *bcdo2* is expressed in ventral cell layers. (**B-E**) At 24 to 32 hpf, *bcdo2* expression is found in anterior parts adjacent to the yolk. (**F**,**G**) At 48 hpf, *bcdo2* is expressed in cardiac and pericardial cells, as well as in endodermal tissues. In G, a higher magnification of the developing heart is shown. (**H**,**I**) Sagittal and transverse cross-sections though the cardiac region reveal expression of *bcdo2* both in the atrium and the ventricle. (**J**) At early larval stages, *bcdo2* is expressed in cells of the (K) gut and (L) liver. Scale bars: 100 μm in A-D,G,J; 50 μm in E,F,H,I,K,L. at, atrium; ve, ventricle.

erythrocytes with fragmented nuclei (supplementary material Fig. S2A,C). Additionally, q-RT-PCR analysis revealed decreased hemoglobin B (*hbbe3*) mRNA levels in *bcdo2* morphants when compared with controls (supplementary material Fig. S2B). Thus, we concluded that knockdown of BCDO2 resulted in apoptosis of blood cells in the zebrafish larva.

4-oxo-4HPR inhibits BCDO2 and recapitulates the blood phenotype *bcdo2* morphants

We have previously shown that the synthetic retinoid fenretinide (4HPR) can inhibit the activity of BCMO1 (Lobo et al., 2010a). BCMO1 accepts carotenoid substrates with a non-modified β-ionone-ring site that is present in 4HPR (Lindqvist and Andersson, 2002). By contrast, BCDO2 displays broad substrate specificity by converting carotenoids with different ring modifications, including ring hydroxylation (Amengual et al., 2011). Thus, we wondered whether the 4HPR derivative 4-oxo-4HPR could inhibit BCDO2 activity. Murine BCDO2 was used for this analysis because this enzyme displayed high enzymatic activity in our in vitro test system (Fig. 5A). Thus, we incubated protein extracts of recombinant BCDO2 with canthaxanthin in the presence of increasing concentrations of 4-oxo-4HPR (Fig. 5B-D). Canthaxanthin, like 4-oxo-4HPR, possesses a 4-oxo-substituted β-ionone ring (Fig. 5C) and is an abundant carotenoid in zebrafish egg yolk (Lampert et al., 2003). BCDO2 efficiently converted canthaxanthin to cleavage products with spectral characteristics of 4-oxo-10′-apocarotenal and rosafluene (Fig. 5B,C) but the conversion rate for canthaxanthin significantly decreased in the presence of increasing amounts of 4-oxo-4HPR (Fig. 5D).

To analyze the effect of 4-oxo-4HPR in vivo, we administered this substance to 2 dpf zebrafish embryos and stained them the next day with o-dianisidine. When compared with the vehicle-only-treated control embryos, 4-oxo-4HPR-treated embryos developed anemia (Fig. 6A). Thus, 4-oxo-4HPR recapitulated the blood phenotype of *bcdo2* morphants, probably by inhibiting BCDO2 activity.

Our previous studies in mice indicated that BCDO2 protects cells against oxidative stress (Amengual et al., 2011). Thus, we next analyzed gene expression of glutathione peroxidase 1 and catalase, which protect erythrocytes against oxidative stress in the fish (Yu et al., 2010). Quantitative real-time PCR with isolated blood cells showed a 3.5- to 7.0-fold increase in mRNA expression levels of these enzymes in 4-oxo-4HPR-treated fish relative to controls (Fig. 6B).

Our whole-mount in situ hybridization experiments did not provide clear evidence that *bcdo2* was expressed in blood cells (Fig. 2). Thus, we used a more sensitive RT-PCR approach for *bcdo2* expression with isolated blood cells. This analysis revealed that Bcdo2 was expressed in the blood (supplementary material Fig. S3A). We then asked whether *bcdo2* expression is also responsive to oxidative stress. To accomplish this, we challenged 2 dpf larvae raised in the absence of PTU with egg water containing 0.03% H_2O_2. After, 24 hours we isolated protein and RNA from these fish and determined BCDO2 protein and mRNA levels. In treated larvae, *bcdo2* expression was increased at the protein and mRNA levels when compared with control siblings (Fig. 6C,D). Additionally, q-RT-PCR analysis of isolated blood cells revealed a 3.3- to 4.1-fold increase of *bcdo2* expression in H_2O_2-treated larvae (supplementary material Fig. S3B). Besides *bcdo2*, the zebrafish genome encodes a putative paralog (annotated as *bcdo2b*) with 59% pairwise amino acid sequence identity. We performed RT-PCR analysis for both *bcdo2* genes with 2 and 3 dpf embryos. *bcdo2b* was not expressed (supplementary material Fig. S3A), thus excluding the possibility that it exerts a developmental role similar to *bcdo2*.

Carotenoids elicit ROS production and decrease ΔΨm in a BCDO2-dependent manner

Our analysis in zebrafish indicated that knockdown of BCDO2 resulted in oxidative stress that damaged cardiac tissue and induced apoptosis in red blood cells. To mechanistically relate BCDO2 to apoptosis, we decided to take advantage of in vitro cell culture systems. Therefore, we screened several human cell lines for BCDO2 expression by immunoblot analysis (Fig. 7A). This analysis revealed that, with exception of HepG2 cells, all tested cell

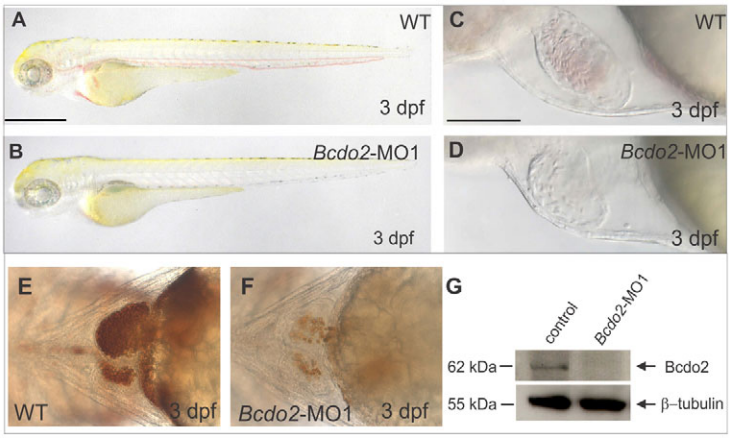

Fig. 3. Targeted knockdown of BCDO2 causes anemia in zebrafish embryos. (**A-D**) Lateral views of 3 dpf larvae; (A-D) *bcdo2* morphants show reduced red coloring of blood. (**E**,**F**) Views of the heart of a control (E) and a *bcdo2* morphant (F) stained for hemoglobin. (**G**) Immunoblot analysis for BCDO2 with protein extracts of 2 dpf control and morphant larvae (n=5 embryos per lane). WT, wild type. Scale bars: 500 μm in A,B; 100 μm in C,D.

lines expressed this enzyme when cultured under standard conditions. We then chose T47D cells and HepG2 cells and treated them with BC or canthaxanthin. After 2 hours of incubation, the carboxy-H_2DCFDA dye was added to detect reactive oxygen species (ROS). In the presence of reactive oxygen species (ROS), this reduced fluorescein compound becomes oxidized and emits a bright green fluorescence. Microscopy showed that treated HepG2 cells showed strong green fluorescence, whereas T47D cells showed no such fluorescence (Fig. 7B).

ROS can result from impairment of mitochondrial respiration. To study the effects of carotenoids on this process, we analyzed mitochondrial membrane potential (ΔΨm) of both cell lines with the JC-1 dye (Reers et al., 1991). When mitochondria have a normal ΔΨm, this dye crosses the membrane and forms J-aggregates that appear red under UV light. By contrast, the dye remains in its monomeric form in the cytoplasm and emits a green fluorescence when mitochondrial respiration is impaired. Thus, vehicle-treated HepG2 cells showed red fluorescence for intact mitochondria, whereas carotenoid-treated HepG2 cells showed strong green fluorescence (Fig. 7C). Conversely, after carotenoid-treatment, T47D cells retained their ΔΨm potential, indicated by strong red JC-1 staining in the mitochondria (Fig. 7C). Hence, we concluded that carotenoids can cause ROS production and reduce ΔΨm in HepG2 cells, whereas these effects were absent in T47D cells, which express endogenous BCDO2.

Carotenoids induce the intrinsic apoptotic pathway in HepG2 cells

ΔΨm is an important indicator of mitochondrial health and loss of ΔΨm can lead to the formation of the mitochondrial permeability transition pore (MPTP) and release of cytochrome c into the cytoplasm (Liu et al., 1996). Thus, we determined the localization of cytochrome c in HepG2 cells by immunocytochemistry and confocal imaging (Fig. 7D). In non-treated HepG2 cells, staining for cytochrome c merged with the staining of COXIV, an intrinsic

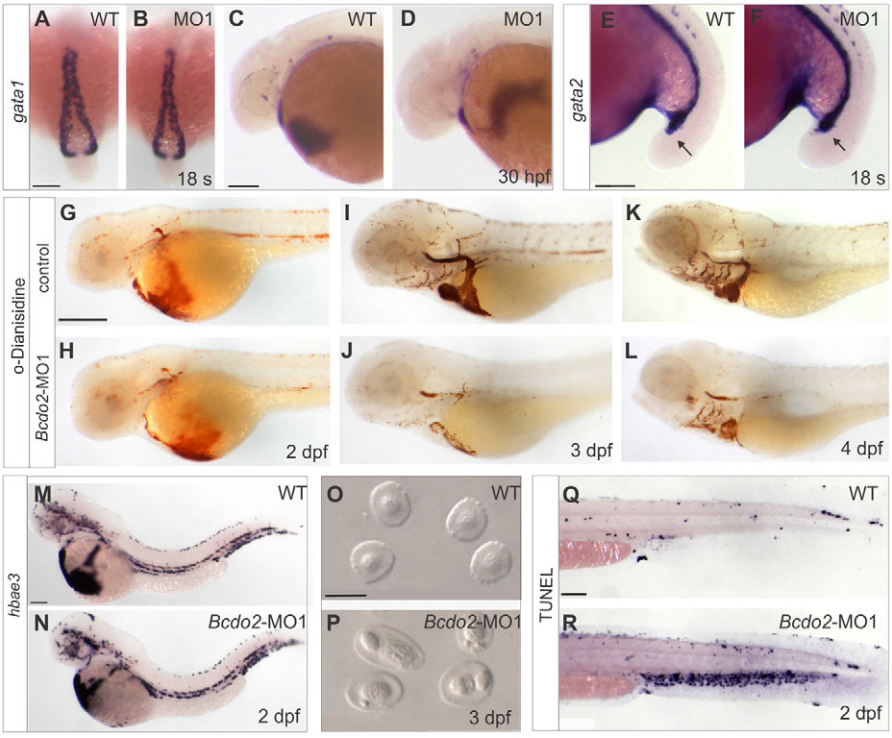

Fig. 4. Characterization of the blood phenotype in *bcdo2* morphant zebrafish larvae. (A,B) Dorsal views, anterior is upwards. (C-N,Q,R) Lateral views. Anterior is towards the left. (**A-F**) Whole-mount in situ hybridization for mRNA expression patterns of *gata1* and *gata2* are similar in morphants and controls. (**G-L**) o-Dianisidine staining for hemoglobin at different developmental stages of control and *Bcdo2* morphant embryos. In 3 dpf *bcdo2* morphants (J), staining is reduced when compared with controls (I). (**M**,**N**) Staining for hemoglobin (*hbae3*) mRNA reveals no differences between 2 dpf *bcdo2* morphants and controls. (**O**,**P**) Blood smears from 3 dpf *bcdo2* morphants and control larvae. Blood cells of *bcdo2* morphants show fragmented nuclei. (**Q**,**R**) TUNEL staining reveals that blood cells of 2 dpf *bcdo2* morphants undergo apoptosis. Scale bars: 100 μm in A-F,M,N,Q,R; 250 μm in G-L; 10 μm in O,P. Whole-mount in situ hybridization experiments were conducted with 30 embryos for each condition. o-Dianisidine staining for hemoglobin in morphant and control siblings was conducted with 50 fish per experiment. The experiment was repeated six times with essentially the same outcome.

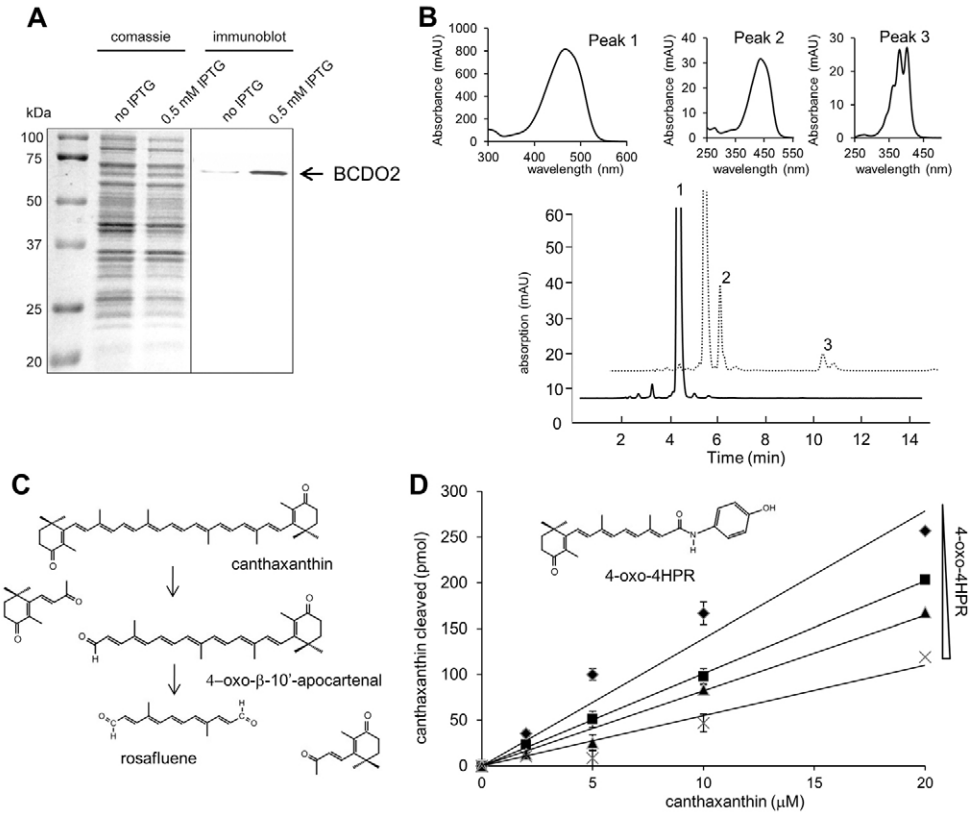

Fig. 5. BCDO2 converts substrates with 4-oxo-ionone ring sites. Recombinant murine BCDO2 was expressed in *E. coli* BL21 cells for 6 hours in the presence or absence of 0.5 mM IPTG. (**A**) 40 mg of protein of non-induced and induced cells were subjected to SDS-PAGE and immunoblot analysis. SDS-PAGE was stained with Coomassie Blue and BCDO2 was detected by an anti-His6 antiserum in immunoblot analysis. (**B**) HPLC profiles at 360 nm of a lipid extract from in vitro tests for BCDO2 enzymatic activity. The reaction was carried out with 20 μM canthaxanthin at 28°C for 10 seconds (solid trace) and 10 minutes (dotted trace). Spectral characteristics of peak 1 (canthaxanthin), peak 2 (4-oxo-β-10′-apocarotenal), peak 3 (rosafluene) are given above the HPLC traces. (**C**) Reaction sequence of canthaxanthin cleavage catalyzed by BCDO2. (**D**) Canthaxanthin cleavage by BCDO2 is inhibited by 4-oxo-fenretinide (4-oxo-4HPR). Recombinant murine BCDO2 was incubated in the presence of increasing concentrations of canthaxanthin in the absence and presence of 4-oxo-4HPR (0 to 5 μM). Reactions were run for 5 minutes at 28°C. In the graph, substrate cleavage (pmol) is plotted versus substrate concentration (μM). Diamonds, no 4-oxo-4HPR; squares, 0.5 μM no 4-oxo-4HPR; triangles, 2 μM no 4-oxo-4HPR; crosses, 5 μM 4-oxo-4HPR. Experiments represent data from three independent experiments. Error bars indicate s.e.m.

mitochondrial marker protein. As expected, in cells treated with H_2O_2, which induces oxidative stress, staining for cytochrome c and COXIV did not merge, indicative of cytochrome c release into the cytoplasm. Importantly, cytochrome c release also was seen in HepG2 cells treated with BC. To demonstrate directly that this process involves MPTP formation, we treated cells with cyclosporine A, a well-described blocker of MPTP (Pastorino et al., 1998). Indeed, cyclosporine A prevented cytochrome c release in cells treated with BC as well as in cells treated with H_2O_2 (Fig. 7D).

Cytochrome c release to the cytoplasm results in the activation of the caspase cascade (Samali et al., 1999). During the execution-phase of apoptosis, pro-caspase 3 undergoes proteolytic processing at conserved aspartic residues to produce two subunits, large (19 kDa) and small (17 kDa), that dimerize to form the active enzyme (Hui et al., 2004). In fact, only pro-caspase 3 was detected by immunoblotting in control HepG2 cells (Fig. 8A). By contrast, HepG2 cells treated with carotenoids exhibited significant proteolytic cleavage of pro-caspase 3 to smaller activated isoforms (Fig. 8A). In carotenoid-treated T47D cells that express BCDO2, no such cleavage of pro-caspase 3 was observed (Fig. 8B). We also measured DNA repair enzymes that are known targets of activated caspase 3. One such enzyme is poly-(ADP) ribose polymerase (PARP1), a 116 kDa protein that plays a role in repair of single-strand DNA breaks (Tewari et al., 1995). Consistent with finding the active cleaved caspase 3 isoforms, we also observed cleavage of PARP1 in HepG2 cells treated with different compounds. Again, no such cleavage was observed in either vehicle-only treated control HepG2 cells or in carotenoid-treated T47D cells that express BCDO2 (Fig. 8A,B).

Biologically active caspase 3 has been found to be responsible for chromatin condensation and DNA fragmentation, which are hallmarks of apoptosis (Zhuang et al., 2007). Using the DNA vital dye Hoechst 33342, we evaluated the effects of different carotenoids and retinoids on chromatin condensation. Blue fluorescent Hoechst 33342 brightly stains the condensed chromatin of apoptotic cells and more dimly stains the normal chromatin of live cells. After treatment with these compounds, HepG2 cells showed a marked increase in blue fluorescence (supplementary material Fig. S4A), whereas T47D cells did not. Cumulatively, these results suggest that through cytochrome c release and activation of caspase 3 and PARP1, carotenoids induced apoptosis in HepG2 cells, whereas T47D cells did not undergo such effects.

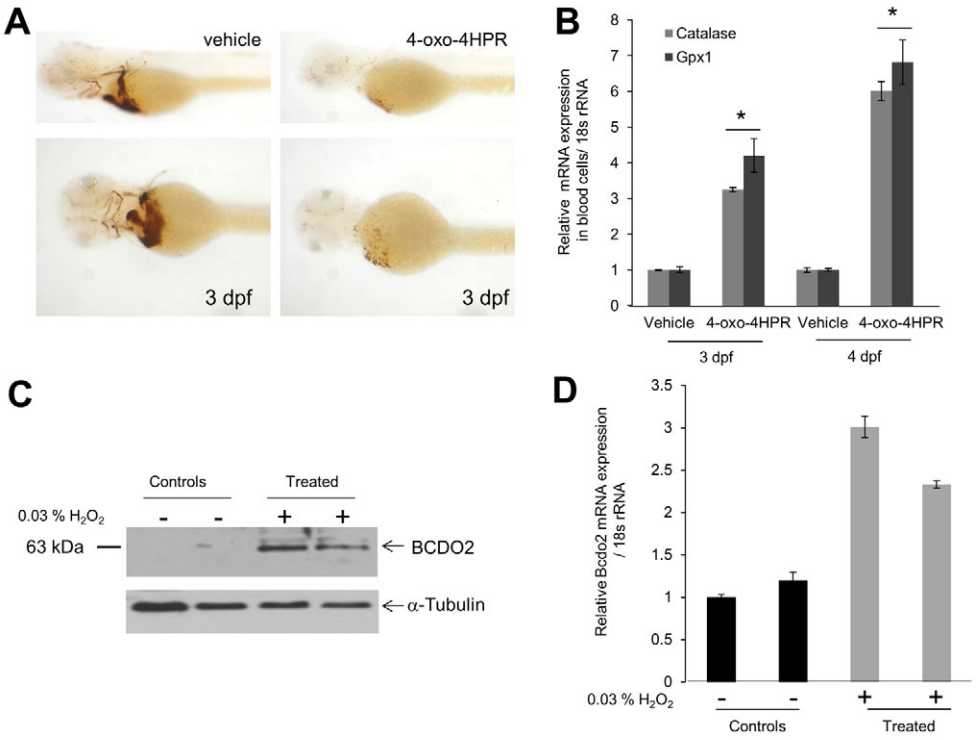

Fig. 6. 4-oxo-fenretinide (4-oxo-4HPR) induces apoptosis of blood cells and oxidative stress in zebrafish larvae. All embryos were raised in the presence of 200 μM 1-phenyl-2-thiourea (PTU) to inhibit pigmentation at 28°C. Two days post-fertilization, embryos (*n*=50 for each condition and experiment) were manually dechorionized and incubated in egg water containing 1 μM 4-oxo-fenretinide (4-oxo-4HPR) or vehicle only [0.1% (v/v) DMSO]. (**A**) After 24 hours, hemoglobin staining was performed using the o-Dianisidine dye. Representative images were taken under a Leica stereo microscope at 1.6× (top panels) and 4.0× (bottom panels) magnifications. (**B**) RNA from isolated blood cells was assessed for glutathione peroxidase 1 (*gpx1*) and catalase mRNA expression. The 18s rRNA probe set was used as the endogenous control. **P*<0.05 compared with controls. Data are mean±s.e.m. (C,D) Larvae (2 dpf) were incubated in the presence or absence of 0.03% hydrogen peroxide (H_2O_2) for 24 hours. (**C**) Protein extracts from 12 larvae per lane were subjected to immunoblot analysis for BCDO2. α-Tubulin was used as protein loading control. (**D**) Total RNA was isolated from 12 larvae and *bcdo2* expression was determined by qRT-PCR. Data are mean±s.e.m.

BCDO2 dictates apoptotic responses to carotenoids and synthetic retinoids in human cancer cells

To finally demonstrate that protection of T47D cells and susceptibility of HepG2 cells against carotenoid-induced apoptosis is strictly dependent on BCDO2 function, we performed a genetics-based experiment. Thus, we treated T47D cells with siRNA directed against *bcdo2* or transiently transfected HepG2 cells with a plasmid encoding murine *bcdo2*. HepG2 cells transiently expressing BCDO2 were then treated with carotenoids and assessed for hallmarks of the intrinsic apoptotic pathway as described above. Our analysis showed a reduction of the carboxy-H_2DCFDA dye fluorescence for HepG2 cells expressing *bcdo2*, when compared with non-transfected HepG2 cells, when challenged with different carotenoids and retinoids (Fig. 8C). Similarly, HepG2 cells expressing BCDO2 showed normally polarized mitochondria membranes, as indicated by strong red fluorescence after JC-1 dye staining (supplementary material Fig. S4B). Finally, immunoblot analyses for cleaved caspase-3 demonstrated that this mediator of apoptosis remained relatively unchanged after treatment of BCDO2-expressing HepG2 cells with carotenoids (Fig. 8D). Conversely, we expected that knockdown of *Bcdo2* by siRNA treatment in T47D cells would enhance ROS production upon carotenoid treatment. This was evidenced by the increase in H_2DFCDA staining when compared with control siRNA untreated cells (Fig. 8E). Interestingly, in T47D cells *Bcdo2* expression was induced by treatment with carotenoids, whereas the *Bcdo2*-specific siRNA decreased *Bcdo2* mRNA levels, as demonstrated by qRT-PCR (supplementary material Fig. S5A,B). More importantly, upon 2 hours of incubation with carotenoids, *bcdo2* siRNA-treated T47D cells showed initiation of apoptosis evidenced by caspase 3 and PARP1 cleavage as established by immunoblot analyses (Fig. 8F). Analysis for chromatin condensation by Hoechst 33342 staining also showed that siRNA-treated T47D cells stained bright blue for condensed chromatin (supplementary material Fig. S4C).

N-acetyl-L-cysteine protects zebrafish erythrocytes from 4-oxo-4HPR-induced apoptosis

Our analyses of human cell lines provided a mechanistic explanation of how carotenoids can induce apoptosis. To translate this finding into the zebrafish model, we determined whether endogenous ROS and apoptosis induction could be abrogated with N-acetyl-L-cysteine (NAC). NAC is an antioxidant with both catalase-like and glutathione reductase-like activities (Yu et al., 2010). Therefore, we treated 2 dpf larvae with 4-oxo-4HPR that can recapitulate the blood phenotype of *bcdo2* morphants in the presence and absence of 5 mM NAC. Then 24 and 48 hours post-treatment, we stained larvae with o-Dianisidine. In 4-oxo-4HPR-only-treated fish we observed a marked reduction in hemoglobin

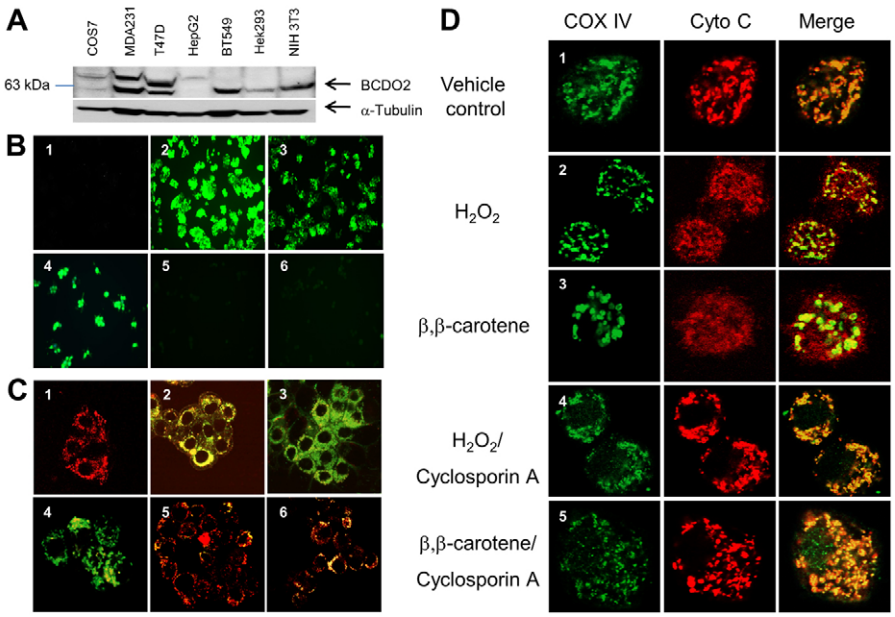

Fig. 7. Carotenoids induce mitochondrial oxidative stress and trigger cytochrome c release in a BCDO2-dependent manner. (**A**) Immunoblot analysis for BCDO2 protein expression in various human cell lines. Note that the BCDO2 antiserum detects an additional protein with higher molecular weight in some cell lines. (**B**) HepG2 cells (panels 1-3) were incubated in the presence of vehicle (panel 1), 1 μM BC (panel 2) and 1 μM canthaxanthin (panel 3). T47D cells (panels 4-6) were incubated in the presence of t-butyl hydroperoxide (panel 4), 1 μM BC (panel 5) and 1 μM canthaxanthin (panel 6). After a 2-hour incubation, the non-fluorescent carboxy-H_2DCFDA dye was added, which (in the presence of reactive oxygen species) emits bright green fluorescence. Data were obtained from three independent experiments. Representative images were obtained with a fluorescence microscope at 20× magnification. (**C**) HepG2 cells (panels 1-3) were incubated in the presence of vehicle (panel 1), 1 μM BC (panel 2) and 1 μM canthaxanthin (panel 3). T47D cells (panels 4-6) were incubated in the presence of the membrane-depolarizing agent carbonylcyanide-m-chlorophenylhydrazone (panel 4), 1 μM BC (panel 5) and 1 μM canthaxanthin (panel 6). After a 2-hour incubation, the mitochondrial membrane potential was assessed by JC-1 staining. Red fluorescence of JC-1 aggregates is indicative of intact mitochondria (panel 1) and green fluorescence of JC-1 monomers dispersed in the cytoplasm indicates mitochondria with depolarized membrane potentials (panel 4). Data were obtained from three independent experiments. Representative images were taken under a confocal microscope at 20× magnification. (**D**) HepG2 cells (rows 1-5) were incubated in the presence of vehicle (row 1), 0.03% hydrogen peroxide (H_2O_2) (rows 2 and 4) and 1 μM BC (rows 3 and 5). Cells in panels 4 and 5 were pre-treated with cyclosporine A. Localization of cytochrome c and the mitochondrial marker protein COXIV was determined by confocal microscopy upon immunostaining at 63× magnification. Cytochrome c, red fluorescence; COXIV, green fluorescence; colocalization of cytochrome c and COXIV, yellow to orange fluorescence.

staining (supplementary material Fig. S6). Conversely, when NAC was added along with 4-oxo-4HPR, these fish were largely protected against this reduction (supplementary material Fig. S6).

DISCUSSION

This study demonstrates a crucial role for the mitochondrial protein BCDO2 in protecting cells against carotenoid-induced oxidative stress and apoptosis (for current model see Fig. 9). We provide evidence in both the zebrafish model and human cell lines that this protective role is directly related to the presence of this oxidative stress inducible mitochondrial protein. Our findings indicate that vertebrates essentially require a mitochondrial carotenoid oxygenase to avoid the detrimental side reactions of carotenoids during embryonic development.

A pathway for the catabolism of carotenoids

BCDO2 belongs to a family of structurally related enzymes that includes RPE65 and BCMO1 (von Lintig et al., 2010). In zebrafish, RPE65a plays a crucial role for ocular vitamin A metabolism (Schonthaler et al., 2007) and BCMO1 is required for retinoic acid production in local tissue compartments (Lampert et al., 2003). BCDO2 was first characterized as a BC and lycopene-metabolizing enzyme (Kiefer et al., 2001). Later, it was shown that this protein also catalyzes oxidative cleavage of carotenoids with 3-hydroxy-ionone rings such as zeaxanthin and lutein (Mein et al., 2011; Amengual et al., 2011). We have demonstrated here that BCDO2 even cleaves canthaxanthin with 4-oxo-substituted ring sites. In this reaction, BCDO2 subsequently removes both ring ends of the carotenoid substrate by cleavage, ultimately resulting in the production of two ionone molecules and the C14-dialdehyde rosafluene.

Several studies proposed that such BCDO2 cleavage products can influence the activities of cell signaling pathways and molecular targets (Mein et al., 2008; Ziouzenkova and Plutzky, 2008). However, this appears problematic because such a broad substrate specificity of BCDO2 would result in the production of numerous metabolites with little specificity. By contrast, BCMO1 displays narrow substrate specificity by exclusively promoting the production of vitamin A (Lindqvist and Andersson, 2002; Maeda et al., 2011). Thus, we propose that BCDO2 is primarily required for carotenoid catabolism. The introduction of oxygen into a parent carotenoid by BCDO2 generates apocarotenoids that can be further metabolized by endogenous enzymes. A mitochondrial retinol dehydrogenase, RDH13, reduces the aldehyde groups of carotenoid-cleavage products to the corresponding alcohols has recently been identified (Belyaeva et al., 2008). A concerted action of BCDO2 with RDH13 would also prevent side reactions of reactive aldehyde groups of the primary cleavage products (Siems

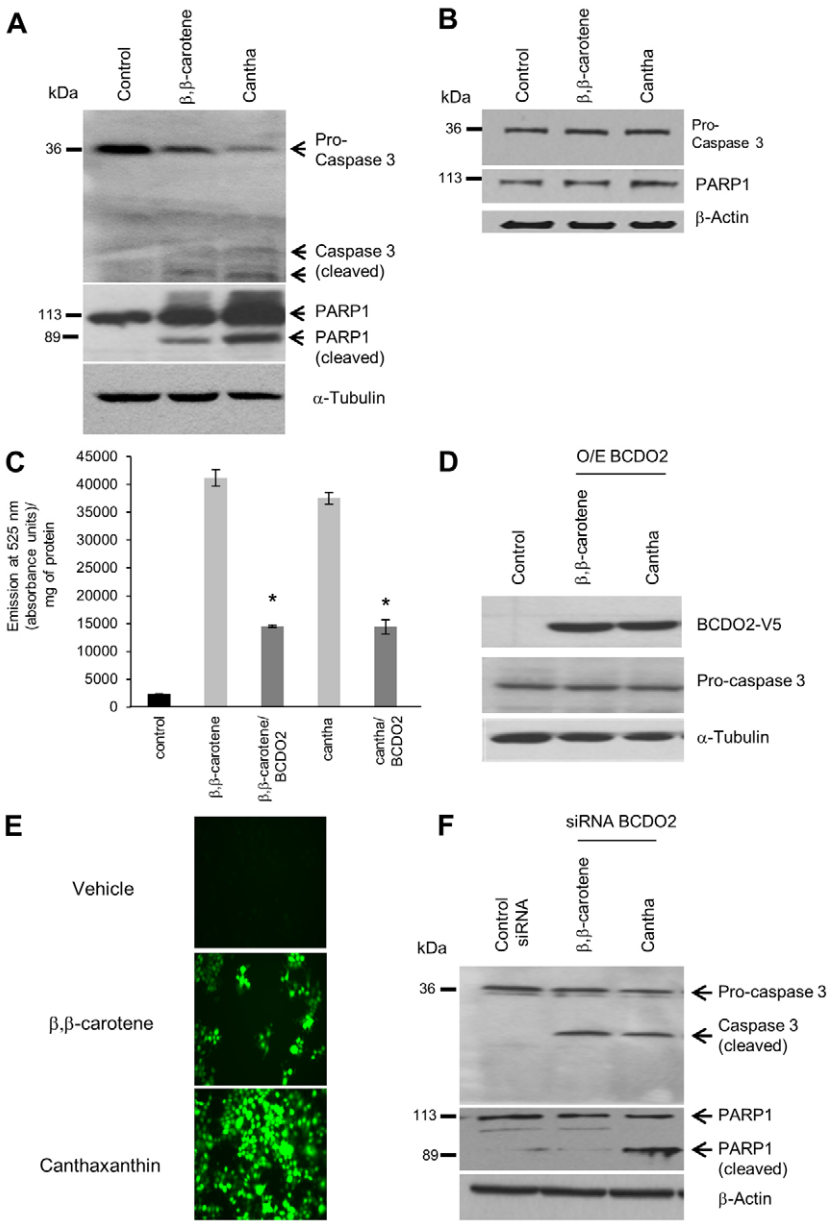

Fig. 8. BCDO2 determines susceptibility of cells to apoptosis induction by carotenoids. (**A**,**B**) HepG2 (A) and T47D (B) cells were incubated in the presence of vehicle, 1 μM BC and 1 μM canthaxanthin. After 2 hours, cells were harvested and protein extracts were subjected to immunoblot analysis using caspase 3 and PARP1 antiserum. (C,D) BCDO2 was expressed as a recombinant protein in HepG2 cells. At 40 hours post transfection, HepG2 cells were incubated in the presence of vehicle, 1 μM BC and 1 μM canthaxanthin, respectively. (**C**) After 2 hours, the non-fluorescent carboxy-H_2DCFDA was added and fluorescence was quantified by emission of light at 525 nm and measured in absorbance units per milligram of protein. Assays were performed in duplicate and repeated three times. **P*<0.05. Data are mean±s.e.m. (**D**) After 2 hours, cells were harvested and protein extracts were subjected to immunoblot analysis using caspase 3 and PARP1 antiserum. (E,F) T47D transfected with siRNA against *bcdo2* were incubated in the presence of vehicle, 1 μM BC and 1 μM canthaxanthin. (**E**) After 2 hours, the H_2DFCDA dye was added. Representative images were obtained with a Leica MM AF fluorescence microscope at 20× magnification. (**F**) After 2 hours, cells were harvested and protein extracts were subjected to immunoblot analysis using caspase 3 and PARP1 antiserum. β-Actin or α-tubulin were used as the protein loading control. Representative immunoblots are shown.

et al., 2002). The apocarotenols then could undergo α-oxidation for further catabolism, as has been described for phytol a structurally related plant isoprenoid (van den Brink and Wanders, 2006).

A BCDO2-dependent pathway for apoptosis induction

An important question is why do vertebrates require a pathway for carotenoid catabolism in mitochondria? Carotenoids are lipids that possess an extended polyene chromophore and can undergo redox and radical reactions (El-Agamey et al., 2004). Mitochondria are membrane-rich structures that bear oxygen-dependent redox systems. We have previously demonstrated in *Bcdo2*$^{-/-}$ mice that abnormal carotenoid level reduces mitochondrial respiration and induces oxidative stress in tissues (Cuperus et al., 2010; Amengual et al., 2011). It is well established that oxidative damage to mitochondria can induce apoptosis of cells (Roberson et al., 1997). Indeed, we found that the susceptibility of cells to induction of apoptosis by carotenoids was largely determined by BCDO2. Thus, HepG2 cells devoid of endogenous BCDO2 were highly susceptible to carotenoid-induced apoptosis, as evidenced by a decrease in mitochondrial membrane potential, activation of caspase 3, cytochrome c leakage from the mitochondria, changes in cellular morphology and eventually chromatin condensation. We also showed that cyclosporine A, which blocks the mitochondrial transition pore, prevented this carotenoid-induced process in HepG2 cells. Moreover, engineered expression of recombinant BCDO2 prevented carotenoid-induced apoptosis of these cells. In a similar fashion, T47D cells expressing endogenous BCDO2 were largely protected against apoptotic responses induced by carotenoids, whereas silencing of *bcdo2* with siRNA made these cells susceptible to apoptosis induction.

The mitochondrial protective role of BCDO2 also was strikingly seen in the developing zebrafish. Knock down of BCDO2 resulted in anemia. Blood cells are highly susceptible to oxidative stress in both zebrafish and mouse models (Yu et al., 2010). Our findings in these fish larvae indicate that mitochondria must be protected

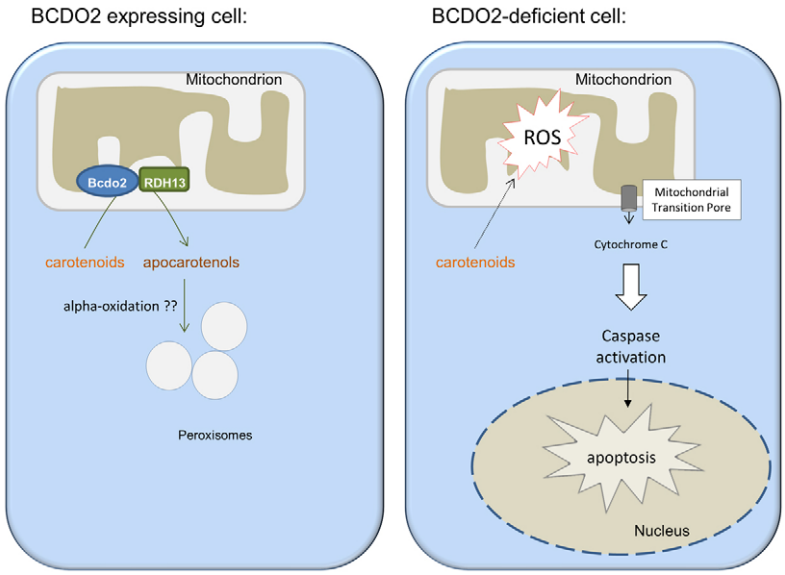

Fig. 9. Schematic overview of the role for mitochondrial BCDO2 in cells. (**A**) Cells that express endogenous or recombinant BCDO2 can degrade carotenoids to apocarotenoids. The primary cleavage products can be further metabolized by RDH13 to the corresponding alcohols. These apocarotenoid alcohols might be then further catabolized by peroxisomal α-oxidation. (**B**) Carotenoids accumulate in the mitochondria in cells which lacking BCDO2 expression. As shown in *Bcdo2*$^{-/-}$ mice, this accumulation interferes with respiration and as shown in this study can induce membrane depolarization and ROS production. These events can cause cytochrome c release and activation of the caspase cascade that eventually leads to apoptosis.

against even low levels of endogenous carotenoids to avoid oxidative stress. A puzzling question is why blood cells are especially vulnerable in BCDO2-deficiency of the fish larva. We think it is unlikely that the putative paralog encoded by the *bcdo2b* gene can protect other tissues against such impairment because this gene was not transcribed during relevant embryonic stages. An explanation for this phenomenon could be that carotenoids are transported in the blood. Thus, blood cells are more exposed to these compounds than other cell types and tissues. The latter assumption may also explain that defects in *bcdo2* morphants occur relatively late in development after a functional circulation has been established. In agreement with a mitochondrial protective role, oxidative stress regulated genes were induced in the blood of larvae treated with the BCDO2 inhibitor 4-oxo-4HPR. Conversely, treatment with the antioxidant NAC prevented anemia in 4-oxo-4HPR-treated fish. Furthermore, we also provided evidence that *bcdo2* is induced in response to oxidative stress. This finding categorizes *bcdo2* as an oxidative stress responsive gene. In the future, it might be worth identifying oxidative stress regulated signaling pathways that target the *Bcdo2* promoter.

General implications for vertebrate carotenoid biology

Our findings establish BCDO2 as a crucial component for zebrafish development. Thus, the question arises as to whether *bcdo2* plays a similar role in other vertebrates. In chicken, a promoter mutation specifically alters *bcdo2* expression in skin but other tissues are not affected (Eriksson et al., 2008). Studies in gold finches indicate that carotenoids can cause adverse health effects when large amounts of these dietary compounds are acquired for the coloration of feathers during molting of male animals (Huggins et al., 2010). In cattle, a putative loss-of-function mutation in *bcdo2* alters BC and retinoid levels in blood and tissues (Berry et al., 2009; Tian et al., 2010). Although one study reports that this mutation has no adverse effects, a second study that analyzed larger populations of different cattle varieties provides evidence that mutations in *bcdo2* are partially recessive. *Bcdo2*$^{-/-}$ mice show impaired mitochondrial function and increased activity of cell signaling pathways related to oxidative stress when challenged with artificial carotenoid rich diets. However, these same *Bcdo2*$^{-/-}$ mice develop normally when raised on vitamin A-rich diets. Notably, intestinal carotenoid absorption is greatly attenuated by dietary retinoids (Lobo et al., 2010b). This characteristic explains why Bcdo2 deficiency does not result in similar effects during mouse embryogenesis (Amengual et al., 2011). A recent study shows that *Bcdo2* is expressed in the mouse embryo and provided a protocol by which mouse embryos can be supplied with carotenoids (Kim et al., 2011). It will be interesting to employ this protocol to further study the effects of carotenoids on embryonic development in a mammalian animal model.

In humans, genetic polymorphisms in *BCMO1* alter carotenoid and retinoid metabolism (Lindqvist et al., 2007; Leung et al., 2008; Ferrucci et al., 2009), but no mutations of *BCDO2* have been described. Clinical studies implicate carotenoids as Janus-faced micronutrients associated with beneficial and adverse health effects. In populations at risk of lung disease, such as smokers, supplementation with BC increased the incidence of cardiovascular disease and lung cancer in large clinical trials (Omenn et al., 1996). Conversely, carotenoids such as lycopene have been associated with chemo-preventive effects against certain forms of cancer (Clinton, 1998). Our findings suggest that both results are associated with mitochondria and BCDO2. Putative cancer-preventing effects might be related to the induction of apoptosis in malignant cells by carotenoids. The reported detrimental consequences might be caused by mitochondrial oxidative stress that induces survival pathways and cell proliferation. It will be fascinating to further explore the role of BCDO2 in various aspects of carotenoid function in health and disease.

Acknowledgements
The authors are grateful to Dr Ruth Keri for providing the breast carcinoma cell lines and to Drs Leslie Webster and Mike Maguire for critical comments and important suggestions on the manuscript.

Funding
This work was supported in part by US National Institutes of Health grants [EY019641, EY020551]. Deposited in PMC for release after 12 months.

Competing interests statement
The authors declare no competing financial interests.

Supplementary material
Supplementary material available online at
http://dev.biologists.org/lookup/suppl/doi:10.1242/dev.079632/-/DC1

References

Agace, W. W. (2008). T-cell recruitment to the intestinal mucosa. *Trends Immunol.* **29**, 514-522.

Amengual, J., Lobo, G. P., Golczak, M., Li, H. N., Klimova, T., Hoppel, C. L., Wyss, A., Palczewski, K. and von Lintig, J. (2011). A mitochondrial enzyme degrades carotenoids and protects against oxidative stress. *FASEB J.* **25**, 948-959.

Belyaeva, O. V., Korkina, O. V., Stetsenko, A. V. and Kedishvili, N. Y. (2008). Human retinol dehydrogenase 13 (RDH13) is a mitochondrial short-chain dehydrogenase/reductase with a retinaldehyde reductase activity. *FEBS J.* **275**, 138-147.

Berry, S. D., Davis, S. R., Beattie, E. M., Thomas, N. L., Burrett, A. K., Ward, H. E., Stanfield, A. M., Biswas, M., Ankersmit-Udy, A. E., Oxley, P. E. et al. (2009). Mutation in bovine beta-carotene oxygenase 2 affects milk color. *Genetics* **182**, 923-926.

Blount, J. D., Metcalfe, N. B., Birkhead, T. R. and Surai, P. F. (2003). Carotenoid modulation of immune function and sexual attractiveness in zebra finches. *Science* **300**, 125-127.

Bone, R. A., Landrum, J. T., Dixon, Z., Chen, Y. and Llerena, C. M. (2000). Lutein and zeaxanthin in the eyes, serum and diet of human subjects. *Exp. Eye Res.* **71**, 239-245.

Chambon, P. (1996). A decade of molecular biology of retinoic acid receptors. *FASEB J.* **10**, 940-954.

Clinton, S. K. (1998). Lycopene: chemistry, biology, and implications for human health and disease. *Nutr. Rev.* **56**, 35-51.

Cuperus, R., Leen, R., Tytgat, G. A., Caron, H. N. and van Kuilenburg, A. B. (2010). Fenretinide induces mitochondrial ROS and inhibits the mitochondrial respiratory chain in neuroblastoma. *Cell. Mol. Life Sci.* **67**, 807-816.

El-Agamey, A., Lowe, G. M., McGarvey, D. J., Mortensen, A., Phillip, D. M., Truscott, T. G. and Young, A. J. (2004). Carotenoid radical chemistry and antioxidant/pro-oxidant properties. *Arch. Biochem. Biophys.* **430**, 37-48.

Ellett, F. and Lieschke, G. J. (2010). Zebrafish as a model for vertebrate hematopoiesis. *Curr. Opin. Pharmacol.* **10**, 563-570.

Eriksson, J., Larson, G., Gunnarsson, U., Bed'hom, B., Tixier-Boichard, M., Strömstedt, L., Wright, D., Jungerius, A., Vereijken, A., Randi, E. et al. (2008). Identification of the yellow skin gene reveals a hybrid origin of the domestic chicken. *PLoS Genet.* **4**, e1000010.

Ferrucci, L., Perry, J. R., Matteini, A., Perola, M., Tanaka, T., Silander, K., Rice, N., Melzer, D., Murray, A., Cluett, C. et al. (2009). Common variation in the beta-carotene 15,15′-monooxygenase 1 gene affects circulating levels of carotenoids: a genome-wide association study. *Am. J. Hum. Genet.* **84**, 123-133.

Ford, N. A., Clinton, S. K., von Lintig, J., Wyss, A. and Erdman, J. W., Jr (2010). Loss of carotene-9′,10′-monooxygenase expression increases serum and tissue lycopene concentrations in lycopene-fed mice. *J. Nutr.* **140**, 2134-2138.

Ford, N. A., Moran, N. E., Smith, J. W., Clinton, S. K. and Erdman, J. W., Jr (2011) An interaction between carotene-15,15′-monooxygenase expression and consumption of a tomato or lycopene-containing diet impacts serum and testicular testosterone. *Int. J. Cancer* **131**, E143-E148.

Hessel, S., Eichinger, A., Isken, A., Amengual, J., Hunzelmann, S., Hoeller, U., Elste, V., Hunziker, W., Goralczyk, R., Oberhauser, V. et al. (2007). CMO1 deficiency abolishes vitamin A production from beta-carotene and alters lipid metabolism in mice. *J. Biol. Chem.* **282**, 33553-33561.

Hu, K. Q., Liu, C., Ernst, H., Krinsky, N. I., Russell, R. M. and Wang, X. D. (2006). The biochemical characterization of ferret carotene-9′,10′-monooxygenase catalyzing cleavage of carotenoids in vitro and in vivo. *J. Biol. Chem.* **281**, 19327-19338.

Huggins, K. A., Navara, K. J., Mendonça, M. T. and Hill, G. E. (2010). Detrimental effects of carotenoid pigments: the dark side of bright coloration. *Naturwissenschaften* **97**, 637-644.

Hui, H., Dotta, F., Di Mario, U. and Perfetti, R. (2004). Role of caspases in the regulation of apoptotic pancreatic islet beta-cells death. *J. Cell. Physiol.* **200**, 177-200.

Isken, A., Golczak, M., Oberhauser, V., Hunzelmann, S., Driever, W., Imanishi, Y., Palczewski, K. and von Lintig, J. (2008). RBP4 disrupts vitamin A uptake homeostasis in a STRA6-deficient animal model for Matthew-Wood syndrome. *Cell Metab.* **7**, 258-268.

Jin, H., Xu, J. and Wen, Z. (2007). Migratory path of definitive hematopoietic stem/progenitor cells during zebrafish development. *Blood* **109**, 5208-5214.

Kiefer, C., Hessel, S., Lampert, J. M., Vogt, K., Lederer, M. O., Breithaupt, D. E. and von Lintig, J. (2001). Identification and characterization of a mammalian enzyme catalyzing the asymmetric oxidative cleavage of provitamin A. *J. Biol. Chem.* **276**, 14110-14116.

Kim, Y. K., Wassef, L., Chung, S., Jiang, H., Wyss, A., Blaner, W. S. and Quadro, L. (2011). β-Carotene and its cleavage enzyme β-carotene-15,15′-oxygenase (CMOI) affect retinoid metabolism in developing tissues. *FASEB J.* **25**, 1641-1652.

Krinsky, N. I., Landrum, J. T. and Bone, R. A. (2003). Biologic mechanisms of the protective role of lutein and zeaxanthin in the eye. *Annu. Rev. Nutr.* **23**, 171-201.

Lampert, J. M., Holzschuh, J., Hessel, S., Driever, W., Vogt, K. and von Lintig, J. (2003). Provitamin A conversion to retinal via the beta,beta-carotene-15,15′-oxygenase (bcox) is essential for pattern formation and differentiation during zebrafish embryogenesis. *Development* **130**, 2173-2186.

Lee, C. M., Boileau, A. C., Boileau, T. W., Williams, A. W., Swanson, K. S., Heintz, K. A. and Erdman, J. W., Jr (1999). Review of animal models in carotenoid research. *J. Nutr.* **129**, 2271-2277.

Leung, W. C., Hessel, S., Meplan, C., Flint, J., Oberhauser, V., Tourniaire, F., Hesketh, J. E., von Lintig, J. and Lietz, G. (2008) Two common single nucleotide polymorphisms in the gene encoding {beta}-carotene 15,15′-monoxygenase alter {beta}-carotene metabolism in female volunteers. *FASEB J.* **23**, 1041-1053.

Lian, F., Smith, D. E., Ernst, H., Russell, R. M. and Wang, X. D. (2007). Apo-10′-lycopenoic acid inhibits lung cancer cell growth in vitro, and suppresses lung tumorigenesis in the A/J mouse model in vivo. *Carcinogenesis* **28**, 1567-1574.

Lieschke, G. J. and Currie, P. D. (2007). Animal models of human disease: zebrafish swim into view. *Nat. Rev. Genet.* **8**, 353-367.

Lindqvist, A. and Andersson, S. (2002). Biochemical properties of purified recombinant human beta-carotene 15,15′-monooxygenase. *J. Biol. Chem.* **277**, 23942-23948.

Lindqvist, A., Sharvill, J., Sharvill, D. E. and Andersson, S. (2007). Loss-of-function mutation in carotenoid 15,15′-monooxygenase identified in a patient with hypercarotenemia and hypovitaminosis A. *J. Nutr.* **137**, 2346-2350.

Liu, X., Kim, C. N., Yang, J., Jemmerson, R. and Wang, X. (1996). Induction of apoptotic program in cell-free extracts: requirement for dATP and cytochrome c. *Cell* **86**, 147-157.

Lobo, G. P., Amengual, J., Li, H. N., Golczak, M., Bonet, M. L., Palczewski, K. and von Lintig, J. (2010a). Beta,beta-carotene decreases peroxisome proliferator receptor gamma activity and reduces lipid storage capacity of adipocytes in a beta,beta-carotene oxygenase 1-dependent manner. *J. Biol. Chem.* **285**, 27891-27899.

Lobo, G. P., Hessel, S., Eichinger, A., Noy, N., Moise, A. R., Wyss, A., Palczewski, K. and von Lintig, J. (2010b). ISX is a retinoic acid-sensitive gatekeeper that controls intestinal beta,beta-carotene absorption and vitamin A production. *FASEB J.* **24**, 1656-1666.

Maeda, T., Perusek, L., Amengual, J., Babino, D., Palczewski, K. and von Lintig, J. (2011). Dietary 9-cis-β,β-carotene fails to rescue vision in mouse models of leber congenital amaurosis. *Mol. Pharmacol.* **80**, 943-952.

Mein, J. R., Lian, F. and Wang, X. D. (2008). Biological activity of lycopene metabolites: implications for cancer prevention. *Nutr. Rev.* **66**, 667-683.

Mein, J. R., Dolnikowski, G. G., Ernst, H., Russell, R. M. and Wang, X. D. (2011). Enzymatic formation of apo-carotenoids from the xanthophyll carotenoids lutein, zeaxanthin and β-cryptoxanthin by ferret carotene-9′,10′-monooxygenase. *Arch. Biochem. Biophys.* **506**, 109-121.

Moise, A. R., von Lintig, J. and Palczewski, K. (2005). Related enzymes solve evolutionarily recurrent problems in the metabolism of carotenoids. *Trends Plant Sci.* **10**, 178-186.

Murayama, E., Kissa, K., Zapata, A., Mordelet, E., Briolat, V., Lin, H. F., Handin, R. I. and Herbomel, P. (2006). Tracing hematopoietic precursor migration to successive hematopoietic organs during zebrafish development. *Immunity* **25**, 963-975.

Nasevicius, A. and Ekker, S. C. (2000). Effective targeted gene 'knockdown' in zebrafish. *Nat. Genet.* **26**, 216-220.

Omenn, G. S., Goodman, G. E., Thornquist, M. D., Balmes, J., Cullen, M. R., Glass, A., Keogh, J. P., Meyskens, F. L., Jr, Valanis, B., Williams, J. H., Jr et al. (1996). Effects of a combination of beta carotene and vitamin A on lung cancer and cardiovascular disease. *N. Engl. J. Med.* **334**, 1150-1155.

Paik, J., During, A., Harrison, E. H., Mendelsohn, C. L., Lai, K. and Blaner, W. S. (2001). Expression and characterization of a murine enzyme able to cleave beta-carotene. The formation of retinoids. *J. Biol. Chem.* **276**, 32160-32168.

Palczewski, K. (2006). G protein-coupled receptor rhodopsin. *Annu. Rev. Biochem.* **75**, 743-767.

Pastorino, J. G., Chen, S. T., Tafani, M., Snyder, J. W. and Farber, J. L. (1998). The overexpression of Bax produces cell death upon induction of the mitochondrial permeability transition. *J. Biol. Chem.* **273**, 7770-7775.

Pevny, L., Simon, M. C., Robertson, E., Klein, W. H., Tsai, S. F., D'Agati, V., Orkin, S. H. and Costantini, F. (1991). Erythroid differentiation in chimaeric mice blocked by a targeted mutation in the gene for transcription factor GATA-1. *Nature* **349**, 257-260.

Redmond, T. M., Gentleman, S., Duncan, T., Yu, S., Wiggert, B., Gantt, E. and Cunningham, F. X., Jr (2001). Identification, expression, and substrate specificity of a mammalian beta-carotene 15,15′-dioxygenase. *J. Biol. Chem.* **276**, 6560-6565.

Reers, M., Smith, T. W. and Chen, L. B. (1991). J-aggregate formation of a carbocyanine as a quantitative fluorescent indicator of membrane potential. *Biochemistry* **30**, 4480-4486.

Roberson, K. M., Penland, S. N., Padilla, G. M., Selvan, R. S., Kim, C. S., Fine, R. L. and Robertson, C. N. (1997). Fenretinide: induction of apoptosis and

endogenous transforming growth factor beta in PC-3 prostate cancer cells. *Cell Growth Differ.* **8**, 101-111.
Samali, A., Cai, J., Zhivotovsky, B., Jones, D. P. and Orrenius, S. (1999). Presence of a pre-apoptotic complex of pro-caspase-3, Hsp60 and Hsp10 in the mitochondrial fraction of jurkat cells. *EMBO J.* **18**, 2040-2048.
Schonthaler, H. B., Lampert, J. M., Isken, A., Rinner, O., Mader, A., Gesemann, M., Oberhauser, V., Golczak, M., Biehlmaier, O., Palczewski, K. et al. (2007). Evidence for RPE65-independent vision in the cone-dominated zebrafish retina. *Eur. J. Neurosci.* **26**, 1940-1949.
Siems, W., Sommerburg, O., Schild, L., Augustin, W., Langhans, C. D. and Wiswedel, I. (2002). Beta-carotene cleavage products induce oxidative stress in vitro by impairing mitochondrial respiration. *FASEB J.* **16**, 1289-1291.
Stachura, D. L. and Traver, D. (2011). Cellular dissection of zebrafish hematopoiesis. *Methods Cell Biol.* **101**, 75-110.
Tewari, M., Quan, L. T., O'Rourke, K., Desnoyers, S., Zeng, Z., Beidler, D. R., Poirier, G. G., Salvesen, G. S. and Dixit, V. M. (1995). Yama/CPP32 beta, a mammalian homolog of CED-3, is a CrmA-inhibitable protease that cleaves the death substrate poly (ADP-ribose) polymerase. *Cell* **81**, 801-809.
Tian, R., Pitchford, W. S., Morris, C. A., Cullen, N. G. and Bottema, C. D. (2010). Genetic variation in the beta, beta-carotene-9′, 10′-dioxygenase gene and association with fat colour in bovine adipose tissue and milk. *Anim. Genet.* **41**, 253-259.
van den Brink, D. M. and Wanders, R. J. A. (2006). Phytanic acid: production from phytol, its breakdown and role in human disease. *Cell. Mol. Life Sci.* **63**, 1752-1765.
von Lintig, J. (2010). Colors with functions: elucidating the biochemical and molecular basis of carotenoid metabolism. *Annu. Rev. Nutr.* **30**, 35-56.
von Lintig, J. and Vogt, K. (2000). Filling the gap in vitamin A research. Molecular identification of an enzyme cleaving beta-carotene to retinal. *J. Biol. Chem.* **275**, 11915-11920.
von Lintig, J., Kiser, P. D., Golczak, M. and Palczewski, K. (2010). The biochemical and structural basis for trans-to-cis isomerization of retinoids in the chemistry of vision. *Trends Biochem. Sci.* **35**, 400-410.
Yu, D., dos Santos, C. O., Zhao, G., Jiang, J., Amigo, J. D., Khandros, E., Dore, L. C., Yao, Y., D'Souza, J., Zhang, Z. et al. (2010). miR-451 protects against erythroid oxidant stress by repressing 14-3-3zeta. *Genes Dev.* **24**, 1620-1633.
Zhuang, S., Yan, Y., Daubert, R. A., Han, J. and Schnellmann, R. G. (2007). ERK promotes hydrogen peroxide-induced apoptosis through caspase-3 activation and inhibition of Akt in renal epithelial cells. *Am. J. Physiol. Renal Physiol.* **292**, F440-F447.
Ziouzenkova, O. and Plutzky, J. (2008). Retinoid metabolism and nuclear receptor responses: New insights into coordinated regulation of the PPAR-RXR complex. *FEBS Lett.* **582**, 32-38.